IOP Publishing Journal of Physics D: Applied Physics

J. Phys. D: Appl. Phys. **40** (2007) 6989–6999 doi:10.1088/0022-3727/40/22/020

Modes of rf capacitive discharge in low-pressure sulfur hexafluoride

V Lisovskiy[1], J-P Booth[2], J Jolly[2], S Martins[3], K Landry[3], D Douai[4], V Cassagne[5] and V Yegorenkov[1]

[1] Kharkov National University, Kharkov 61077, Ukraine
[2] Laboratoire de Physique et Technologie des Plasmas, Ecole Polytechnique, Palaiseau 91128, France
[3] Unaxis Displays Division France SAS, 5, Rue Leon Blum, Palaiseau 91120, France
[4] Association Euratom-CEA, Département de Recherches sur la Fusion Contrôlée, CEA Cadarache, F-13108 Saint Paul lez Durance Cedex, France
[5] Riber, 31 rue Casimir Périer, 95873 Bezons, France

E-mail: lisovskiy@yahoo.com

Received 2 August 2007, in final form 20 September 2007
Published 2 November 2007
Online at stacks.iop.org/JPhysD/40/6989

Abstract

This paper presents the results of an experimental study of rf capacitive discharge in low-pressure SF_6. The rf discharge in SF_6 is shown to exist not only in weak-current (α-) and strong-current (γ-) modes but also in a dissociative δ-mode. This δ-mode is characterized by a high degree of SF_6 dissociation, high plasma density, electron temperature and active discharge current, and it is intermediate between α- and γ-modes. The δ-mode appears due to a sharp increase in the dissociation rate of SF_6 molecules via electron impact starting after a certain threshold value of rf voltage. At the same time the threshold ionization energy of SF_x ($x = 1$–5) radicals formed is below the ionization potential of SF_6 molecules. The double layer existing in the anode phase of the near-electrode sheath is shown to play an important role in sustaining the α- mode as well as the δ-mode but it is not a cause of the rf discharge transition from α- to δ-mode.

1. Introduction

Sulfur hexafluoride (SF_6) is a man-made gas which is used by the electric power industry, in semiconductor processing, as a blanket gas for magnesium refining, as a reactive gas in aluminium recycling to reduce porosity, for thermal and sound insulation, and in voice communication, leak checking, atmospheric trace gas studies, ball inflation, etc [1].

Rf capacitive discharge in SF_6 is widely applied in technological processes of etching silicon-based materials [2,3], GaAs [4], treatment of polyethylene films [5] and textile [6], cleaning walls of technological vessels from etching or deposition products [7], etc. Therefore a large number of papers are devoted to studying rf discharge in SF_6 both in experiment and in theory. Let us make a brief review of the main results obtained by other authors, which are directly related to the results of our paper.

Kakuta *et al* [8] experimentally investigated electrical characteristics of rf discharges in SF_6 and in its mixtures with N_2. Space- and time-resolved emission spectroscopy was used to gain a better understanding of kinetics of processes leading to various observed characteristics. In voltage–current dependences at 13 MHz two distinct regions were observed similar to the α to γ transitions observed for electropositive gases. But ionization by secondary electrons is not supported by spatiotemporal emission measurements. The discharge appeared more resistive. Nakano *et al* [9] numerically predicted the radical transport to the surface of narrow-gap reactive ion etcher in SF_6 and investigated the spatiotemporal structure of discharge. The functionality of the narrow-gap rf discharge in SF_6 is due to the appearance of a double layer in front of the instantaneous anode. The maintenance of the rf discharge is accomplished by ionization at the double layer. Okuno *et al* [10] studied potential structures in radio frequency (13.56 MHz) discharges containing negative ions (SF_6 in He gas) in an asymmetrical electrode system using an emissive probe. A double layer type potential profile was found near an instantaneous anode unlike the almost flat profile in He plasma.

Foest *et al* [11] investigated rf discharge in pure SF_6 using GEC reference cell. They obtained that the plasma becomes more resistive as pressure increased. The optical emission intensity had pronounced peaks in front of the powered electrode and a complex double layer formation at the plasma-sheath boundary, which can be attributed to the strong electron-attaching properties of the gas. A significant fraction (as much as 80% in some cases) of the SF_6 in the cell can be dissociated or decomposed when the discharge was on. Koike *et al* [12] studied the decomposition characteristics and etching performances of CF_4, SF_6 and NF_3 in their plasma. Within the range of delivered power under study the decomposition ratio for SF_6 did not exceed 5–6%.

Here we cited only a small portion of published papers devoted to rf discharge in SF_6. An impression may be created that the rf discharge in SF_6 was already studied in such detail that there is no necessity of further research. However, only papers [8, 11] deal with the discharge burning modes and the transition between them. The authors of papers [8, 11] made an assumption that the presence of a sharp increase of the discharge current with rf voltage growing was due to significant increase of ionization at the double layer in the near-electrode sheaths, and, as a consequence, to the increase of the rf electric field in the discharge volume. At the same time, the authors of [8,11] present only a limited set of current–voltage characteristics (CVCs) (the paper [8] gives the CVCs for the SF_6 pressure values of 0.1, 0.5 and 1 Torr, and the authors of [11] limited themselves only to a single CVC for the SF_6 pressure value of 0.1 Torr). It is difficult to understand what occurs with a CVC on varying the pressure; what are the modes of discharge existence under various conditions. In our opinion, the authors of [8, 11] made erroneous conclusions on the burning modes of rf discharge in SF_6. Moreover, there are discrepancies in evaluating the dissociation degree of SF_6 molecules in the discharge: paper [11] reports the values up to 80%, whereas the authors of [12] made a statement about a low dissociation degree, not exceeding 6%. Therefore, a complete understanding of physical processes in rf discharge in SF_6 is obviously still missing.

As is known [13–22] an rf capacitive discharge may exist in a weak-current (α-) and a strong-current (γ-) modes. The authors of papers [13–19] made an assumption that in a weak-current α-mode the electrons acquired their energy required for ionizing gas molecules oscillating in an rf electric field within the plasma volume. However, papers [20, 21] using the fluid modelling demonstrate that in a weak-current α-mode the electrons fill the near-electrode sheath during its anode phase. In the cathode phase the expanding boundary of the sheath sweeps the electrons into the plasma, at the same time, they may gain energy from the electric field in the sheath. The authors of papers [20, 21] call the weak-current α-mode a 'wave riding mode'. The modelling also shows that the ionization rate of gas molecules via electrons swept by the expanding boundary of the sheath exceeds considerably that made by electrons gaining their energy only in the rf field in the plasma volume. In a strong-current γ-mode electron avalanches develop in near-electrode sheaths resulting in the enhanced ionization rate near sheath boundaries.

This paper shows that the increase in the discharge current with rf voltage growing is not caused by increasing ionization at the double layer in the near-electrode sheaths but by the transition of the rf discharge from a weak-current mode to a dissociative (δ-) mode, with a higher degree of gas molecule dissociation. This regime is not a strong-current one but it possesses a high plasma density and a strong discharge current. The dissociative δ-mode is observed starting from a certain threshold value of the rf voltage across the electrodes, when a sufficient number of high energy electrons capable of dissociating SF_6 molecules appear in the discharge. The SF_x-radicals generated possess low ionization potentials, and they play a role of an admixture which is easy to ionize, thus increasing the ionization rate in the discharge.

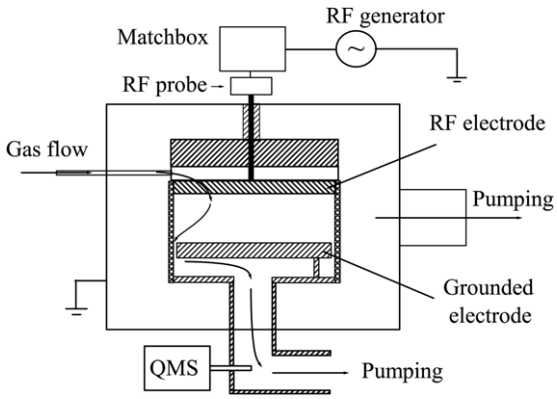

Figure 1. Schematic of the first experimental set-up.

2. Description of the experiment

Experiments were conducted on two research devices.

In our first research device (see figure 1) the capacitive rf discharge was ignited at the frequency of rf field $f = 13.56$ MHz. The experiments were conducted with SF_6 within the gas pressure range $p \approx 0.02$–2 Torr with the inter-electrode distance values of $d = 25$ mm and $d = 20.4$ mm. Parallel-plate aluminium electrodes had the diameter of 143 mm. The rf voltage with the amplitude $U_{rf} < 1000$ V from the generator was fed through the matchbox to the potential electrode while another electrode was grounded. Electrodes were located inside the fused silica tube with the inner diameter of 145 mm. The gas under study was fed into the inner chamber through small orifices in one electrode and then pumped out through the gap between the second electrode and the wall of the fused silica tube. This discharge chamber was completely surrounded with a grounded grid and put inside a large grounded chamber with the diameter of 315 mm and the height of 231 mm (see figure 1). The grounded grid, the fused silica tube around the electrodes and a lower gas pressure (by 1–2 orders of magnitude) in the large chamber prevented the ignition of the self-sustained rf discharge in it. The outer chamber possessed a sufficiently large window of fused silica enabling one to observe the discharge behaviour in the process of cleaning the inner chamber.

Rf voltage U_{rf} was measured with the rf voltage-current probe (rf probe Z'SCAN, Advanced Energy). This rf probe was located at the minimum possible distance from the rf electrode. Z'SCAN permitted to register not only the values of rf voltage, rf current, phase shift angle φ between current

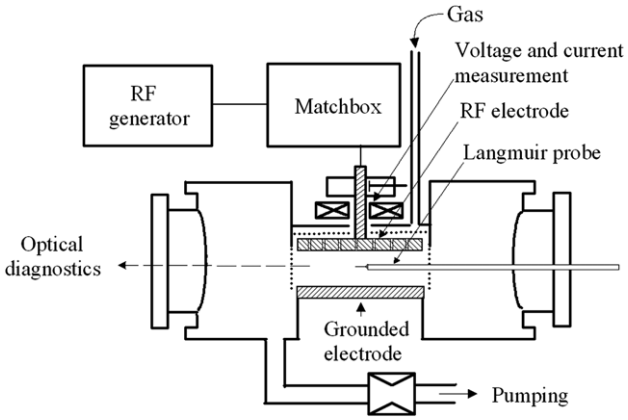

Figure 2. Schematic of the second experimental set-up.

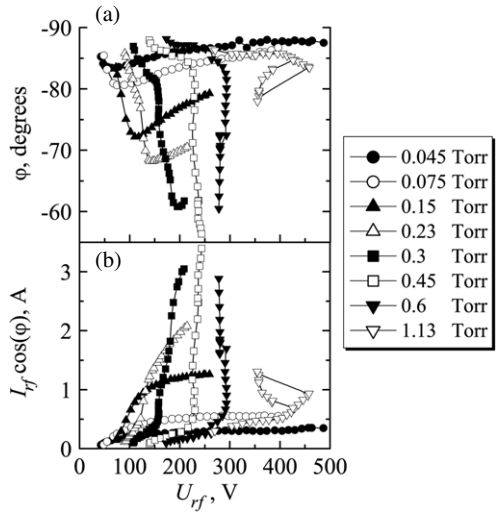

Figure 3. Phase shift angle between rf current and voltage (*a*) and active rf current (*b*) against applied rf voltage. SF_6, $L = 25$ mm.

and voltage and delivered power for the basic frequency but also the values of rf current and voltage for harmonics. We used the RF5S rf generator (RF Power Products Inc.) with the maximum delivered power of 500 W and the PFM matching box (Huettinger Elektronik GmbH) of L-type. In a number of experiments a more powerful (up to 2000 W) rf generator (Advanced Energy) was also used.

Gas pressure was monitored with 10 and 1000 Torr capacitive manometers (MKS Instruments). The gas flow was set to 5 sccm with a mass flow controller (sccm denotes cubic centimetre per minute), and the pressure was regulated by throttling the outlet to the pump. The adaptive pressure controller supported the constant value of the gas pressure (in those cases when it was kept constant in the process of measurements).

The QMS 421 (Balzers) quadrupole mass-spectrometer analysed the content of the neutral gas leaving the discharge chamber (in the downstream). The gas under analysis was fed from the system of the chamber pumping out through a narrow capillary what permitted to perform gas analysis up to the pressures order of 1 Torr.

In another research set-up (see figure 2) the experiments were carried out within the gas pressures range $p = 0.1$–0.6 Torr in the range of rf voltage amplitude values $U_{rf} \leqslant 500$ V and the rf field frequency $f = 13.56$ MHz. The rf discharge was sustained between two parallel-plate electrodes of 12 cm in diameter and a discharge gap of 3 cm width. Electrical rf power at a given frequency was produced via a signal generator (Marconi Instruments) connected to a 150 W power amplifier (Amplifier Research, 150A220). The rf voltage was applied to the upper electrode through an L-type matching network mounted directly on the reactor. The back of the powered electrode was shielded with a grounded counter-electrode. The lower electrode was grounded and the plasma was confined to the inter-electrode volume by a cylindrical stainless-steel grid fixed to the counter-electrode. The voltage and current were measured using a calibrated rf coupler (Coaxial dynamics 87004) and a current probe (Eaton 91550), installed on the power lead close to the rf electrode, and recorded using a digital oscilloscope. The rf power delivered by the rf amplifier was measured by an inline power meter situated between the amplifier and the matchbox. The area of the rf electrode was two times less than the area of grounded surfaces (electrode and grid). The flow rate of SF_6 was 30 sccm, and the oxygen flow rate was 3 sccm, controlled by an upstream mass flow controller. Oxygen was added into the discharge volume to prevent sulphur deposition on the Langmuir probe surface.

Electron temperature T_e and plasma potential were determined from a single cylinder platinum probe (6 mm long and 0.18 mm in diameter), located at the discharge centre, with the probe axis parallel to the electrode surface. The Langmuir probe (SmartProbe from Scientific Systems) was rf compensated at 13.56 MHz. The compensation electrode (the reference probe) had the area of 3.5 cm^2, the shunt capacitance was equal to 50 pF. The blocking impedance of the probe circuit was larger than 100 KΩ for 13.56 MHz. The electron temperature T_e was determined from the CV probe characteristics (from the inclination angle of the linear section of the probe electron current plotted in a semi-logarithmic scale). Because of numerous types of positive ions present in the discharge volume in SF_6 (SF_5^+, SF_3^+, F^+) [38], it becomes rather difficult to determine the plasma density n_i from the ion branch of the probe current I_{pr}.

The visible radiation issuing from the discharge centre was directed with lenses onto the slit of the monochromator equipped with a photoelectric multiplier. The line intensities of atomic fluorine and oxygen corresponding to the wavelengths of 7037.5 Å and 7770 Å, respectively, were recorded.

3. Experimental results

Consider first the results we have obtained with the first set-up for the inter-electrode gap of $L = 25$ mm. Figure 3 shows phase shift angle φ between rf current and voltage and active rf current $I_{rf}\cos(\varphi)$ against the rf voltage amplitude for various SF_6 pressure values. The figure presents eight current–voltage characteristics within the SF_6 pressure range $p = 0.045$–1.13 Torr (we registered in total 22 CVCs within this pressure range).

It is better to start the discussion of the results presented in figure 3 with the curves for higher pressure values. With the sufficiently large SF_6 pressure of $p \approx 1$ Torr the rf

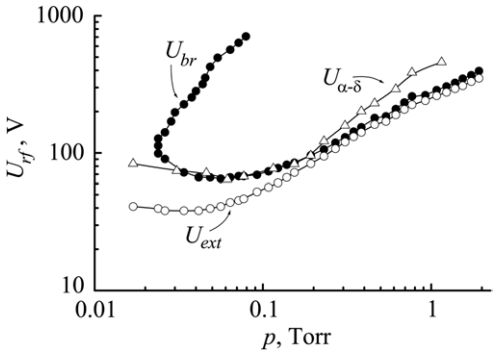

Figure 4. Breakdown curve, extinction curve and α–δ transition curve. SF_6, $L = 25$ mm.

discharge at low values of delivered power (tens of watts) is burning first in a clearly weak-current (α) mode, its CVC being positive (the active current is observed to increase with rf voltage growing). After the rf voltage approaches some critical value the discharge contracts jump-like into a column (constricted discharge), whose CVC is negative (it was proved earlier, e.g. by Ogle and Woolsey [23]). Probably, at large SF_6 pressures the constricted discharge corresponds to the strong-current (γ) mode of the rf discharge (its characteristics: rf current amplitude, phase shift angle, active rf current and delivered power $P_{\rm dlv}$ differ drastically from those of the weak-current mode). When we now decrease the SF_6 pressure then we will see that within the pressure range $p \approx 0.2$–0.6 Torr the weak-current mode: (1) exists in a more narrow range of rf voltage and (2) experiences a transition to a mode with a sharp growth of the rf current with a comparatively small increase of the rf voltage. This mode (let us call it tentatively a δ-mode) is not similar to the strong-current γ-mode, but, at the same time, it can hardly be attributed to a weak-current mode because of the exceedingly large value of the active rf current (several amperes). At the rf voltage corresponding to the α–δ transition, the CVC exhibits a characteristic dogleg feature permitting to observe the α–δ transition even at the lowest gas pressure values we studied. Spatiotemporal excitation wave forms and current–voltage transients indicate that the transition is not to the so-called γ-mode [8].

We can report the visual observations of the three modes we observed. The discharge luminosity in the weak-current mode uniformly covered the total surface of the electrodes in the pressure range studied. The dissociative mode also appeared visually as uniform. The strong-current mode was uniform at low pressure. Then the appearance of a more brightly shining column near the chamber axis surrounded by the uniform luminosity was observed at the pressure above 0.6 Torr. And at the pressure above 1 Torr the strong-current mode was burning in the form of a brightly shining column.

Figure 4 shows the breakdown curve $U_{\rm br}(p)$, the extinction curve $U_{\rm ext}(p)$ and the transition curve from α-mode to δ-mode $U_{\alpha-\delta}(p)$. The breakdown curve of the rf capacitive discharge in SF_6, similar to other gases [13, 24–27], possesses a multi-valued section of the rf breakdown voltage dependence on gas pressure. In contrast to nitrogen and hydrogen [27], the extinction curve in the high SF_6 pressure range (>0.3 Torr) runs very close to the breakdown curve, the breakdown voltage exceeding the extinction voltage by only 15–25 V (what is associated, probably, with a strong attachment property of SF_6 molecules). It follows from the figure that the weak-current mode may exist only within the narrow range of rf voltage values $U_{\rm rf}$ between the extinction curve $U_{\rm ext}$ and the transition curve from α-mode to δ-mode $U_{\alpha-\delta}$. At higher rf voltages the discharge was burning in δ-mode, and only at voltage values exceeding 450 V the strong-current γ-mode can be observed.

Figure 5 depicts the rf current, phase shift angle, active rf current and delivered power against gas pressure for several fixed values of the rf voltage (with $U_{\rm rf} > U_{\alpha-\delta}$). The amplitude of the rf current, active rf current and delivered power possess maxima (phase shift angle possesses a minimum), to the left of which the discharge is burning in δ-mode, whereas to the right (at higher SF_6 pressure) we observe the weak-current (α) mode. The more is the rf voltage value, the sharper is the variation of the rf discharge characteristics on increasing the SF_6 pressure and experiencing a transition to the weak-current α-mode.

With the help of the quadruple mass-spectrometer we recorded the mass-spectra of the gas mixture downstream the discharge gap under various conditions. Figure 6 shows the mass-spectra of the weak-current α-mode and δ-mode. It is clear from the figure that the mass-spectrum of the α-mode consists of the SF_5^+, SF_4^+, SF_3^+, SF_2^+, SF^+, as well as S_2^+ peaks. After the transition of the rf discharge to δ-mode the SiF_3^+ peak appeared in the mass-spectrum characterizing the product of silicon reacting with fluorine SiF_4 . Probably, SiF_4 could appear in our chamber as a result of etching the walls of the fused silica tube with fluorine generated due to dissociation of SF_6 molecules.

The peaks of SF_5^+, SiF_3^+ and S_2^+, whose dependence on rf voltage is depicted in figure 7 are the most interesting for us here. Our aim is to estimate the dissociation degree of SF_6 molecules in the rf discharge in various modes of burning. Obviously we have to treat the SF_5^+ peak characterizing the concentration of SF_6 molecules. The intensity of the S_2^+ peak also points to the dissociation degree because sulphur molecules can be produced only after complete dissociation of SF_6 molecules. The SiF_3^+ peak is also very important because it indicates the rate of etching a wall of the fused silica tube with fluorine atoms and molecules. The chemically active fluorine has time to react with the electrode surface, wall of the fused silica tube, to recombine with SF_x radicals on the walls, and, as a result, a conventional mass-spectrometer shows peaks of F^+ and F_2^+ formed within itself under ionization of SF_6 molecules. But we can get the information on the presence of fluorine atoms and molecules in the discharge from the intensity of SiF_3^+ peak, because the more fluorine is produced due to dissociation of SF_6 molecules, the faster is the rate of etching the surface of the fused silica tube, and the larger is the concentration of the final SiF_4 product of etching.

As we see from figure 7, the intensity of SF_5^+ peak in α-mode slowly increases with the rf voltage growing, and after the transition to δ-mode within the range of $U_{\rm rf} = 205$–230 V about 1.5 times decrease of SF_5^+ peak is observed. The intensities of SiF_3^+ and S_2^+ peaks in α-mode decrease weakly, but after the transition to δ-mode the intensities of these peaks within the same range of rf voltage are 10 and 3 times larger, respectively.

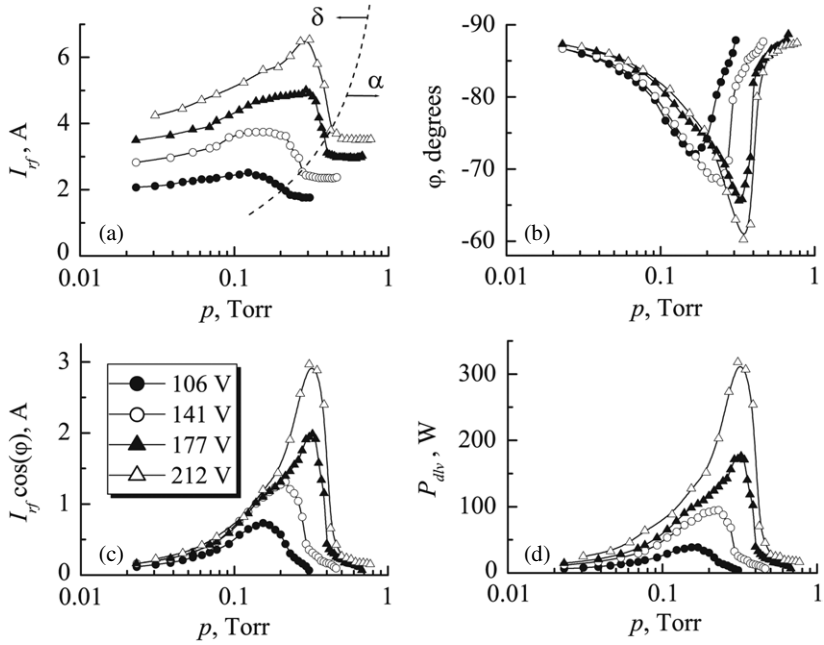

Figure 5. Rf current amplitude (*a*), phase shift angle between rf current and voltage (*b*), active rf current (*c*) and delivered power (*d*) against SF_6 pressure, $L = 25$ mm.

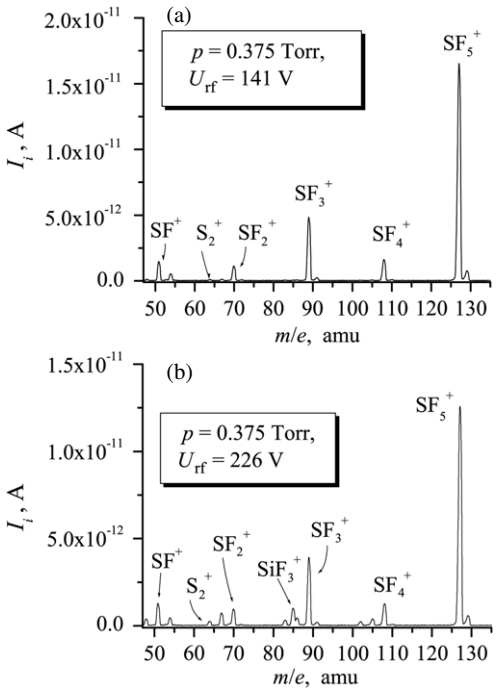

Figure 6. Gas mass-spectra downstream for (*a*) α-mode, $U_{rf} = 141$ V and (*b*) δ-mode, $U_{rf} = 226$ V. SF_6, $L = 25$ mm, $p = 0.375$ Torr.

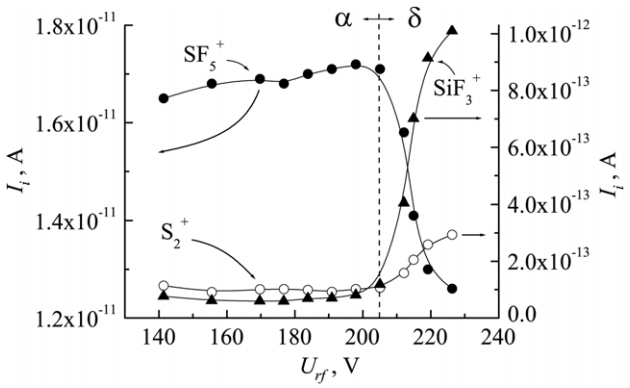

Figure 7. SF_5^+, SiF_3^+ and S_2^+ peak intensities against applied rf voltage for the inter-electrode gap of $L = 25$ mm and SF_6 pressure of $p = 0.375$ Torr.

Let us evaluate the dissociation degree of SF_6 molecules from formulae [11]:

$$D_u = \frac{I_0(SF_5^+) - I_{pl}(SF_5^+)}{I_0(SF_5^+)}, \quad (1)$$

$$D_l = \frac{I_0(SF_5^+) - I_{pl}(SF_5^+)}{I_0(SF_5^+) + I_{pl}(SF_5^+)}, \quad (2)$$

where I_0 and I_{pl} are the intensities of the SF_5^+ without and with the rf discharge, respectively. Here D_u denotes the upper limit of the dissociation degree of SF_6 molecules and it is found under the assumption that the total gas number density does not increase with dissociation. As in our set-up a gas input flow rate and pressure are kept constant during the experiment, then the excessive number of radicals formed under dissociation of gas molecules are partly removed out of the discharge chamber, at the same time the adaptive pressure controller opens the throttle valve to maintain constant pressure. The lower limit of the dissociation degree of SF_6 molecules D_l is obtained under the assumption that each molecule dissociates only into two radicals, and that the excessive increase of gas pressure is decreased via opening the throttle valve. It can be expected that the true value for the dissociation fraction lies between the limits D_u and D_l [11].

The values D_u and D_l we obtained are shown in figure 8, where the CVC (I_{rf} cos(φ)) can also be observed. It is clear

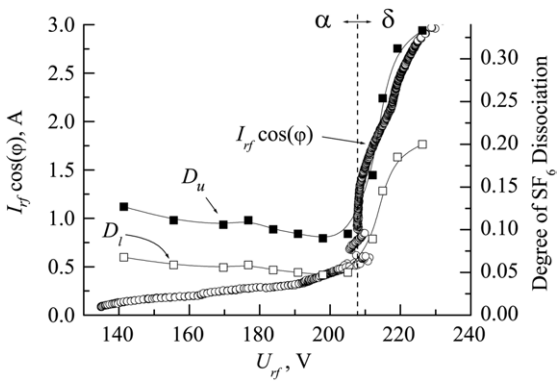

Figure 8. Rf active current and dissociation degrees D_u and D_l for SF_6 molecules against applied rf voltage, $L = 25$ mm, $p = 0.375$ Torr.

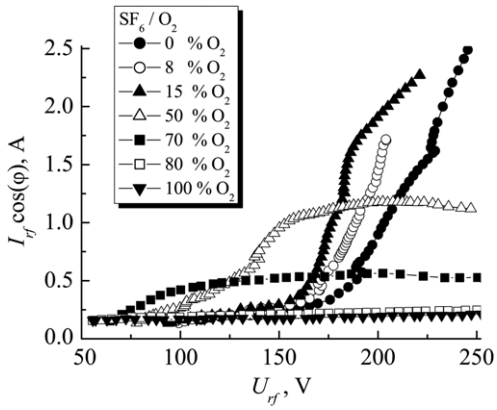

Figure 9. Active rf current against applied rf voltage for various oxygen admixture amount to SF_6, $L = 15$ mm.

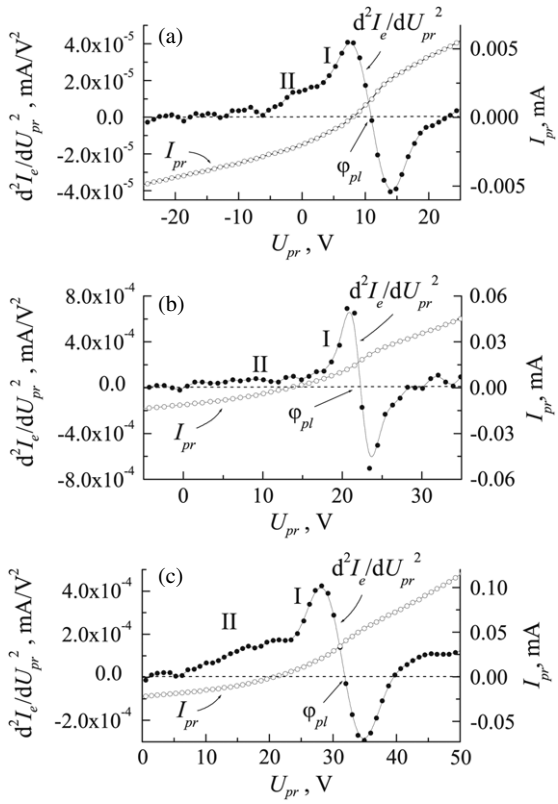

Figure 10. Probe CVCs I_{pr} (U_{pr}) and electron probability distribution functions d^2I_{pr}/dU_{pr}^2 for the inter-electrode gap of $L = 30$ mm, pressure of the $SF_6 + O_2$ mixture of $p = 0.3$ Torr and applied rf voltage values: (*a*) $U_{rf} = 159$ V, α-mode, (*b*) $U_{rf} = 226$ V, α-mode, (*c*) $U_{rf} = 254$ V, δ-mode.

from the figure that a slow increase in the conductance current with rf voltage growing in α-mode is accompanied with a small decrease in the dissociation degree of gas molecules. When the rf voltage approaches a certain threshold value, the discharge experiences a transition to δ-mode, the conductance current starts to increase sharply with the dissociation degree of gas molecules also increasing considerably. So, when the discharge current experiences 6-time increase (within a certain range of rf voltages) the dissociation degree increases around 4-fold.

As we said above, we performed our experiments in two discharge chambers differing in design. In the first chamber the inter-electrode gap and gas feed were $L_1 = 2.5$ cm, $Q_1 = 5$ sccm, whereas in the second one the values were $L_2 = 3$ cm, $Q_2 = 30$ sccm $SF_6 + 3$ sccm O_2. However, not only the rf voltage values of α–δ transition ($U_{rf.1} \approx 226$ V and $U_{rf.2} \approx 230$ V at gas pressure 0.5 Torr) happened to be close to each other but also the rf current amplitude values ($I_{rf.1} \approx 3.7$ A and $I_{rf.2} \approx 3.5$ A), corresponding to this transition. We added oxygen into the second chamber to prevent the sulphur film deposition on the surface of the Langmuir probe. Figure 9 shows CVCs for various oxygen admixture values to SF_6. It follows from this figure that moderate (to 15%) oxygen admixtures lead to a moderate decrease in the rf voltage of the α–δ transition, but the δ-mode itself is expressed under these conditions just as well as in pure SF_6.

The second experimental device permitted to perform probe measurements of inner characteristics of the discharge (electron temperature T_e and constant plasma potential), as well as to study the optical radiation from the central region of the discharge in α- and δ-modes. Figure 10 depicts the probe CVCs I_{pr} (U_{pr}) and the second derivatives of the probe electron current with respect to probe voltage d^2I_e/dU_{pr}^2 (electron energy probability functions, EEPFs). Figure 10(*a*) shows the results for α-mode near the rf discharge extinction, whereas figure 10(*b*) presents the results for α-mode just before the transition to δ-mode, and figure 10(*c*) presents those for δ-mode. Conventionally the EEPF of the rf discharge contains two groups of electrons: the group of 'cold' electrons I possessing approximately a maxwellian distribution with temperature T_e, and a EEPF tail of high energy electrons II. Increasing the rf voltage leads to a considerable decrease in the width of 'cold' electrons I indicating the decrease in electron temperature, but the number of 'cold' electrons increases uniformly. At the same time, the number of high energy electrons in the second group II also increases, the 'tail' of the group II spreading to higher energy. After transition to δ-mode, the width of the group of 'cold' electrons I and the number of high energy electrons in the second group II increase.

Figure 11 shows the rf current amplitude I_{rf}, electron temperature T_e, dc plasma potential φ_{pl}, as well as the line intensities of atomic fluorine I_F (7037.5 Å) and atomic oxygen I_O (7770 Å) against rf voltage. At the smallest rf voltage values (before rf discharge extinction) electron temperature is high

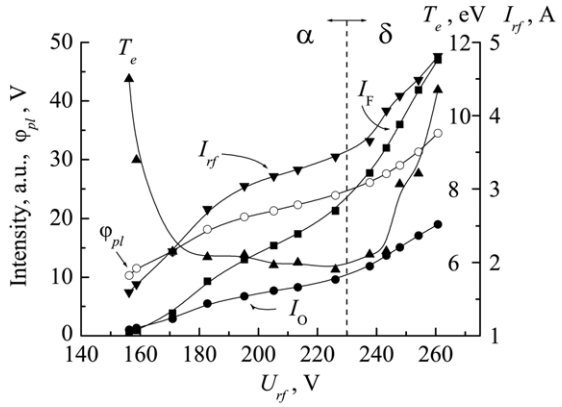

Figure 11. Rf current amplitude, electron temperature, dc plasma potential, radiation intensities of atomic fluorine and oxygen against applied rf voltage, $L = 30$ mm, pressure of the $SF_6 + O_2$ mixture of $p = 0.3$ Torr.

(order of 8–11 eV), dc plasma potential equals about 10 V, and the discharge glow is weak. Increasing the rf voltage is accompanied, first, with an abrupt decrease in electron temperature, which then up to the transition from α- to δ-mode decreases weakly, and it amounts to 6 eV. The intensities of the lines I_F and I_O increase uniformly, the dc plasma potential growing as well. After the transition of the discharge to δ-mode the electron temperature experiences fast increase with rf voltage growing, the intensities of the lines I_F and I_O also growing faster.

The discharge CVCs for the first device presented in figure 3 were recorded with the rf generator with the maximum power of 500 W. In order to clarify the situation, we performed a set of recordings with the first device using the rf generator capable to deliver 2000 W, the inter-electrode gap being equal to $L = 20.4$ mm. Figure 12 shows our results (rf active current, phase shift angle as well as delivered power). Using this generator we managed to get not only α- and δ-modes, but to approach γ-mode in a number of cases. Consider the CVC for SF_6 pressure of $p = 0.4$ Torr, shown in figure 13, in more detail. In section AB we observe α-mode, the discharge current being small and less than 0.2 A. After the rf voltage approached the value 216 V, the discharge transits to δ-mode; the slow increase of the rf voltage is accompanied by a fast growth of the rf active current and delivered power, the near-electrode sheath thickness decreases considerably. However, the discharge still possesses the structure similar to α-mode, but its glow is more intense. At the same time the violet tint of the glow in the vicinity of near-electrode sheath boundaries usually inherent to γ-mode, is not observed in this case. When the rf voltage approaches the value of 385 V, an abrupt jump of the discharge occurs from point C to point D (see figure 13). We did not manage to fix the rf voltage, say, at 500 V, because this state was unstable. However our rf probe Z'SCAN permitted to perform up to 32 recordings per second. During the period the discharge required to perform a transition from point C to point D we managed to make one-two recordings. In figure 13 section CD was constructed from 14 CVCs, recorded for identical conditions. In section DE the discharge clearly is burning in γ-mode, judging from violet glow near sheath boundaries, indicating the presence of fast electrons accelerated in near-electrode sheaths.

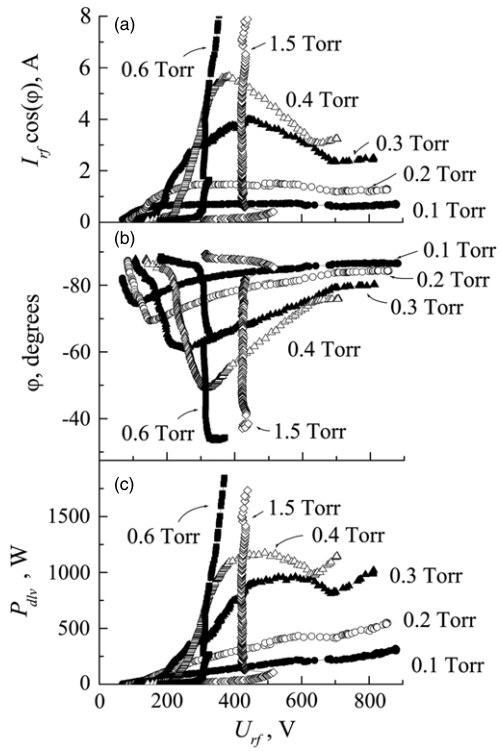

Figure 12. Rf active current (a), phase shift angle between rf current and voltage (b) and delivered power (c) against applied rf voltage for different SF_6 pressure values, $L = 20.4$ mm.

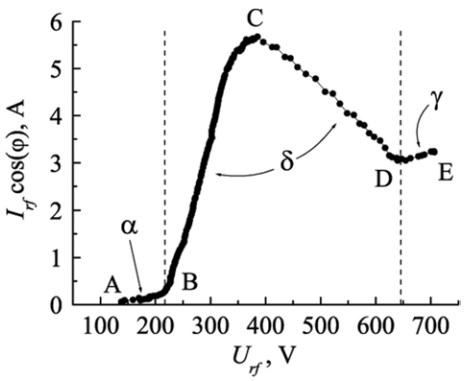

Figure 13. Rf active current against applied rf voltage for SF_6 pressure of $p = 0.4$ Torr and $L = 20.4$ mm.

The transition from δ-mode to γ-mode occurs when the rf voltage applied across the electrodes approaches a critical value at which electron avalanches develop in the near-electrode sheath. It means that the sheath becomes to be conductive, and a flow (beam) of high energy electrons goes out of it into the plasma volume. These fast electrons may carry a remarkable part of the discharge current. A similar situation is observed in the dc discharge where a flow of fast electrons leave the cathode sheath and a negative glow and Faraday dark space are located next to the cathode sheath. There is no necessity to support a strong electric field in these two regions because the current is transported by fast electrons as well as by diffusion. We can assume that the transition of the rf discharge to γ-mode takes place as follows. Probably the appearance of the flow of fast electrons from the sheath

of the rf discharge also leads to the decrease of the rf field in the plasma volume. In γ-mode the quasi-neutral plasma is transformed into two negative glows (adjacent to near-electrode sheaths) and two dark Faraday spaces overlapping in the central region of the discharge gap. Owing to this fact the electron temperature in the plasma decreases, and the dissociation rate of SF_6 molecules via electron impact falls. This circumstance decreases the concentration of easily ionized radicals in the discharge volume, what together with the lowering of the electron temperature gives rise to a considerable decrease in the ionization rate in plasma. The decrease in the dissociation degree of SF_6 molecules lowers the attachment rate of electrons to radicals and free fluorine atoms; the concentration of negative ions drops, what according to [8], leads to the decrease in the rf electric field in plasma. Decreasing the rf plasma field leads to lowering the rf voltage drop across the quasi-neutral plasma and increasing the rf voltage drop across the near-electrode sheaths. The number and energy of fast electrons in the beam grow and the rf field in the plasma lowers again. As a result we have the lowered concentrations of positive and negative ions and free electrons in plasma, what we observe as a sharp decrease of the rf discharge current under δ–γ transition. At low SF_6 pressure this transition occurs smoothly without jumps of the discharge current because the dissociation degree of SF_6 molecules in the δ-mode does not exceed 10%. With the growth of pressure the dissociation degree in the δ-mode increases, and an abrupt decrease in the dissociation degree in the γ-mode gives rise to a jump-like δ–γ transition. Note that the picture of the δ–γ transition we suggest needs a check through numerical simulation.

4. Discussion

Thus, what is δ-mode and why does it appear? The authors of papers [8, 11] made an attempt to attribute the presence of an abrupt increase of the discharge current with rf voltage growing (under α- to δ-mode transition) to the increasing of the role of double layers formed in the anode phase in near-electrode sheaths. Moreover, the authors of [8] say: 'An additional ionization channel opens when local E/N, most probably in the double layer, reaches the value where the ionization rate is greater than attachment. This mechanism, similar to dc breakdown, leads to a sudden increase of current and reduction of impedance. We can explain the observed transition as being the result of significant increase of ionization at double layer.' Thus, they assume that the ionization at double layers is weak in α-mode, and only when rf voltage approaches a certain threshold value, 'the local breakdown' of double layers takes place and leads to an abrupt change of discharge characteristics. However in paper [28] the authors conclude that the double layer is involved in a major sustaining mechanism *at the minimum sustaining condition* under all frequencies investigated. That is, the ionization at double layers plays an important role also before the discharge extinction, i.e. in α-mode. It can be observed even with a naked eye that a brightly shining layer exists inside the near-electrode in α-mode (that probably is the above-mentioned double layer [8, 11]). This layer also exists after the transition from α- to δ-mode; at the same time, it may glow even brighter

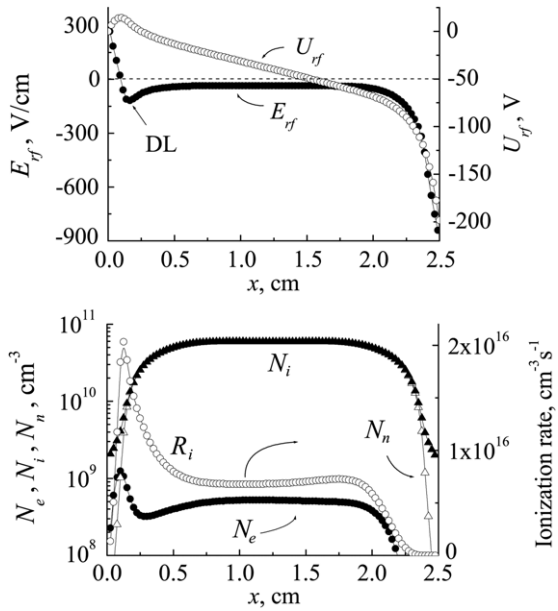

Figure 14. Axial profiles of rf potential U_{rf}, rf electric field E_{rf}, concentrations of electrons N_e, positive N_i and negative N_n ions as well as of the ionization rate at $p = 0.375$ Torr, $U_{rf} = 200$ V for the time moment when the potential of the rf electrode is equal to $U_{el} = -200$ V.

than the plasma in the vicinity of the near-electrode sheath boundary or at the discharge centre.

The presence of the double layer in α-mode can also be seen from the results of our simulation for SF_6, $p = 0.38$ Torr, $U_{rf} = 200$ V (see figure 14). To this end we employed the well-known Siglo-RF code (Kinema Software, http://www.siglo-kinema.com/siglo-rf.htm). This code does not take into account secondary emission from the electrode surface, and one cannot determine from it the parameters of the α–γ transition. It also does not take into account the dissociation and cannot be applied for studying the δ-mode. We used the Siglo-RF code only for calculating axial profiles of plasma parameters in the α-mode. Figure 14 shows the case when the left and right electrodes are instantaneous anode and cathode, respectively. At this instant the left sheath is in the anode phase, i.e. electrons move in the rf field to the left electrode filling the sheath near it. As is clear from figure 14, a double layer is observed inside the left near-electrode sheath. The rf field in the plasma volume is equal to $E_{rf} = 34.7\,\mathrm{V\,cm^{-1}}$, $E_{rf}/p = 92.5\,\mathrm{V\,cm^{-1}\,Torr^{-1}}$. As it follows from Bolsig code (Kinema Software), just at this value of the ratio E/p the ionization rate of gas molecules ν_i is equal to the attachment rate ν_a. In the region of the double layer the rf electric field approaches the value $E_{rf} = 119\,\mathrm{V\,cm^{-1}}$, with $E_{rf}/p = 317\,\mathrm{V\,cm^{-1}\,Torr^{-1}}$. At such E/p value the Bolsig code furnishes $\nu_i \approx 2.07 \cdot \nu_a$. Even in α-mode an intensive ionization takes place within the double layer with the ionization rate exceeding the attachment rate twice. Therefore the transition to the dissociative regime could hardly be explained as a 'local breakdown' within the double layer region because in α-mode the double layer is already 'broken down'. The authors of papers [8, 9, 28–36] obtained similar U, E and N_e profiles for the anode phase of the near-electrode sheath of the rf discharge in electronegative gases.

In the rf discharge positive ions come to the electrode surface in the form of the almost constant current I_i, modulated with the rf field frequency. Electrons can approach the electrode surface only at the anode phase of the sheath, the electron current I_e to the electrode having the pulsed form [36]. The total numbers of positive ions and electrons hitting the electrode surface during the rf field period must be equal. In the rf discharge in electropositive gases this condition is easily met, because in plasma $N_i \approx N_e$. However, in electronegative gases in plasma we have $N_e \ll N_i$. For example, we obtain from figure 14 at the centre of the discharge $N_e \approx 5.24 \times 10^8\,\mathrm{cm}^{-3}$, $N_i \approx 5.97 \times 10^{10}\,\mathrm{cm}^{-3}$, $N_n \approx 5.92 \times 10^{10}\,\mathrm{cm}^{-3}$, i.e. $N_e/N_n \approx 8.85 \times 10^{-3}$. Consequently, the majority of electrons in the discharge volume are attached to SF_6 molecules forming negative ions, and they cannot get to the electrode surface and compensate the positive charge. Therefore at the anode phase of the sheath, when the remaining free electrons are moving to the electrode, a double layer appears in the near-electrode sheath. It is the double layer that heats electrons locally, increasing the ionization rate abruptly and generating the required additional flow of electrons to the electrode. Only in this case the number of positive and negative charges hitting the electrode surface during the rf field period can be equal. Therefore the double layer in the anode phase of the near-electrode sheath must appear in the rf discharge containing negative ions.

As we see, the double layer plays an important role in α-mode as well as in δ-mode. Consequently, the double layer must exist in α-mode as well as in δ-mode and cannot be the cause of the transition of the rf discharge from α- to δ-mode. In our opinion, the gas molecule dissociation via electron impact is the cause of this transition. To coin the notation of δ-mode we took the first letter of the Greek word '$\delta\iota\alpha\sigma\pi\alpha\sigma\eta$' ('diaspasis'), which is translated as 'dissociation' in the sense of breaking a complicated molecule into constituent parts (atoms, radicals).

Thus, in the weak-current α-mode the dissociation degree of SF_6 molecules is small not exceeding 5–10%, what agrees with the results of paper [12]. The temperature of group I electrons decreases weakly with rf voltage growing, however, at the same time, the number of electrons in group II, as well as their energy increase (see figure 9). At some threshold value of the rf voltage we have a sufficiently large number of high energy electrons whose collisions with SF_6 molecules may lead to their dissociation. At the same time, the energy of these electrons is insufficient for ionizing molecules. Ionizing SF_6 molecules via electron impact occurs according to the following scenario:

$$SF_6 + e \rightarrow SF_5^+ + F + 2e, \tag{3}$$

where the threshold energy for ionizing SF_6 molecules is 15.5 eV [37]. However, for dissociating SF_6 molecules,

$$SF_6 + e \rightarrow SF_5 + F + e, \tag{4}$$

$$SF_6 + e \rightarrow SF_4 + 2F + e, \tag{5}$$

$$SF_6 + e \rightarrow SF_4 + F_2 + e, \tag{6}$$

remarkably lower threshold values 9.6 eV, 12.1 eV and 11.3 eV, respectively, are required [37]. Besides, the threshold ionization energies of the radicals formed also happen to be below 15.5 eV, required for ionizing SF_6 molecules:

$$SF_5 + e \rightarrow SF_5^+ + 2e, \tag{7}$$

$$SF_4 + e \rightarrow SF_4^+ + 2e, \tag{8}$$

$$SF_3 + e \rightarrow SF_3^+ + 2e, \tag{9}$$

$$SF_2 + e \rightarrow SF_2^+ + 2e, \tag{10}$$

$$SF + e \rightarrow SF^+ + 2e, \tag{11}$$

and for the processes (7)–(11) they are, respectively, 11.7 eV, 13.0 eV, 10.6 eV, 12.8 eV and 14.7 eV [37] (in paper [38] for processes (7) and (9) the threshold energy values of 11.2 eV and 11.0 eV, respectively, were obtained).

Thus, when rf voltage approaches some threshold value and the discharge possesses a sufficient number of high energy electrons, the dissociation rate of gas molecules via electron impact increases abruptly. At the same time, the radicals possessing a lower ionization potential comparing with SF_6 molecules play the role of an easily ionized admixture to SF_6. Increasing the concentration of radicals induces the growth of their ionization rate via electron impact what leads to the increase of plasma density and conduction current of the rf discharge. A kind of 'positive feedback' takes place in the δ-mode, because an increase in the conduction current brings about an increase in SF_6 dissociation degree and then the increase in SF_6 dissociation degree leads to an increase in the conduction current. This 'positive feedback' process makes the sharp increase in the conduction current after the onset of the δ-mode. Besides, the radicals, as well as fluorine atoms and molecules produced under SF_6 dissociation, may attach free electrons what also involves the growth of the concentration of negative ions. Increasing the concentration of negative ions leads to the increase of the rf electric field in the quasi-neutral plasma to ensure the rf current transport through the plasma volume as well as sustainment of the required ionization rate of gas molecules and radicals by scarce free electrons. According to paper [8], increasing the concentration of electronegative molecules in a gas together with that of negative ions makes an rf discharge more resistive what we see under abrupt transition to the regime with an enhanced dissociation degree. Therefore δ-mode of the rf discharge is characterized by a high plasma density, increased electron temperature and high active current. Similar to α-mode, a double layer has to exist in the anode phase of near-electrode sheaths in δ-mode. The transition of the discharge from δ- to γ-mode may occur at higher rf voltage values when in the near-electrode sheaths electron avalanches develop.

It is clear from the mass-spectra we registered (figure 6), that the ignition of the weak-current mode of the rf discharge and the subsequent α–δ transition are accompanied by a decrease in the concentration of the SF_x radicals. These radicals may participate in various chemical reactions in the discharge volume as well as on the surface of the electrodes and chamber walls. Decrease in the radical concentration with the increase in the power deposited in the discharge, especially under the transition to δ-mode, is probably associated with a strong heating of the gas within the inter-electrode gap. The adaptive pressure controller supported the constant value of the gas pressure. To keep the constant pressure under gas heating the adaptive pressure controller increased the pumping rate of

the gas out of the discharge chamber. At the same time the radicals formed in the dissociation process of SF_6 molecules were also partly pumped out. Therefore for evaluation of the dissociation degree of SF_6 molecules we used the direct measurements of the SF_5^+ peak in the mass-spectrum as well as SiF_3^+ and S_2^+ peaks.

Note that SiF_4 molecules appearing due to etching the fused silica tube in the first chamber by free fluorine can hardly be regarded as an easily ionized admixture, as the ionization potential of such molecules is equal to 15.7 eV [39]. Besides in our second chamber the silicon-containing materials were absent but the δ-mode was observed. Therefore SiF_4 molecules hardly play an important role in the onset of the δ-mode. Atomic and molecular sulphur play a noticeable role in the δ-mode burning, because the ionization potentials of S and S_2 are equal, respectively, to 10.4 eV and 10.7 eV [40].

As was shown in [8], the sharp growth of the discharge current (the discharge transition from weak-current α-mode to δ-mode) is not accompanied by the appearance of electron avalanches in the near-electrode sheath. The spatiotemporal profiles of optical emission in δ-mode do not contain an additional peak near an instantaneous cathode that corresponds to gas molecule excitation via fast secondary electrons coming out of the electrode surface and acquiring a large energy during their motion through the sheath. Therefore, in spite of the high value of the discharge current, δ-mode is not a strong-current γ-mode, because electron avalanches do not develop in the cathode phase of the near-electrode sheath.

Thus, it is expedient to consider three different modes of the rf capacitive discharge in SF_6: a weak-current α-mode, a dissociative δ-mode and a strong-current γ-mode. In the weak-current α-mode the ionization of gas molecules is accomplished by electrons swept out of the near-electrode sheath by its moving boundary [20, 21]. In the dissociative δ-mode the dissociation of gas molecules and the subsequent ionization of the radicals formed is accomplished by the electrons having acquired their energy due to Joule heating in the rf electric field in the plasma volume. In the strong-current γ-mode the electron avalanches developing within the near-electrode sheaths dominate as a source of charged particles. At the same time, however, the breakdown of near-electrode sheaths may not occur [26].

Note that the discharge transition from α- to δ-mode takes place when the ratio of the delivered power P_{dlv} to the gas pressure p approaches a threshold value amounting to $P_{\mathrm{dlv}}/p = 100 \pm 20\,\mathrm{W\,Torr^{-1}}$. It corresponds to the power per unit square of the electrode being $P_{\mathrm{dlv}}/pS = 0.62 \pm 0.12\,\mathrm{W\,Torr^{-1}\,cm^{-2}}$. The rf active current is about 0.37 ± 0.05 A, and the discharge current density is $j_{\mathrm{rf}} = 2.3 \pm 0.34\,\mathrm{mA\,cm^{-2}}$. The authors of paper [8] established that the discharge transition from α-mode to a more resistive mode occurred at $j_{\mathrm{rf}} \approx 2\,\mathrm{mA\,cm^{-2}}$ (that is observed in figure 6 [8]), therefore the threshold value of the discharge current density we obtained is in good agreement with the data of paper [8].

The δ-mode may be called 'dissociative' because the dissociation of gas molecules via electron impact is the most important process in it. This mode is not a unique feature of the rf discharge in SF_6. Moreover, just in SF_6 it is comparatively weakly expressed. It is observed most clearly in SiH_4 and especially in NF_3. As we have shown in another paper [41], under the transition of δ-mode a complete dissociation of NF_3 molecules into radicals occurs that can be easily ionized. At the same time, we observe not just a faster growth of the discharge current with the rf voltage increasing (as in SF_6), but a negative differential conductivity appears, i.e. a growth of the discharge current is accompanied by a considerably decrease of the rf voltage, and the discharge becomes more resistive because a large number of electronegative fluorine atoms are freed. Talking only on α-mode, it is difficult to describe such behaviour of CVCs without introducing a new, dissociative δ-mode.

5. Conclusions

We performed the experimental study of rf capacitive discharge in low-pressure sulfur hexafluoride via recording CVCs, gas mass-spectra downstream and determining inner plasma parameters (electron temperature, plasma potential, electron probability distribution functions) with a probe technique. We also registered the intensity of the optical radiation of the discharge at several wavelengths. It was established that the rf discharge in SF_6 may exist in three different modes: weak-current α-mode, strong-current γ-mode and dissociative δ-mode, the latter being intermediate between α- and γ-modes. The dissociative δ-mode is characterized by a high degree of SF_6 molecule dissociation via electron impact, high electron temperature, plasma density and active rf current of the rf discharge. The dissociative mode sets on starting with a certain threshold rf voltage when the rf discharge possesses a sufficient number of high energy electrons capable to induce dissociation when colliding with SF_6 molecules. At the same time, the ionization potentials of newly formed radicals SF_x ($x = 1$–5) are remarkably lower than the ionization potential for SF_6 molecules, therefore these radicals play the role of an easily ionized admixture to SF_6. The double layer existing in the anode phase of near-electrode sheaths is an important factor of rf discharge sustainment in α- and δ-modes, but it is not the cause of the discharge transition from α- to δ-mode.

References

[1] Christophorou L G, Olthoff J K and Van Brunt R J 1997 *IEEE Electr. Insulation Mag.* **13** 20

[2] Moreau W M 1988 *Semiconductor Lithography: Principles, Practices, and Materials* (New York: Plenum)

[3] Shul R J and Pearton S J 2000 *Handbook of Advanced Plasma Processing Techniques* (Berlin: Springer)

[4] Nordheden K J, Upadhyaya K, Lee Y-S, Gogineni S P and Kao M-Y 2000 *J. Electrochem. Soc.* **147** 3850

[5] Leonard D, Bertrand P, Khairallah-Abdelnour Y, Arefi-Khonsari F and Amouroux J 1995 *Surf. Interface Anal.* **23** 467

[6] Riccardi C, Barni R, Fontanesi M, Marcandalli B, Massafra M, Selli E and Mazzone G 2001 *Plasma Sources Sci. Technol.* **10** 92

[7] Ullal S J, Singh H, Daugherty J, Vahedi V and Aydil E S 2002 *J. Vac. Sci. Technol.* A **20** 1195

[8] Kakuta S, Petrovic Z Lj, Tochikubo F and Makabe T 1993 *J. Appl. Phys.* **74** 4923

[9] Nakano N, Petrovic Z Lj and Makabe T 1994 *Japan. J. Appl. Phys.* **33** 2223

[10] Okuno Y, Ohtsu Y and Fujita H 1994 *Phys. Lett.* A **193** 94

[11] Foest R, Olthoff J K, Van Brunt R J, Benck E C and Roberts J R 1996 *Phys. Rev.* E **54** 1876

[12] Koike K, Fukuda T, Fujikawa S and Saeda M 1997 *Japan. J. Apl. Phys.* **36** 5724
[13] Levitskii S M 1957 *Sov. Phys.—Tech. Phys.* **2** 887
[14] Raizer Y P, Shneider M N and Yatsenko N A 1995 *Radio-Frequency Capacitive Discharges* (Boca Raton, FL: CRC Press)
[15] Yatsenko N A 1981 *Sov. Phys.—Tech. Phys.* **26** 678
[16] Lisovskiy V A 1998 *Tech. Phys.* **43** 526
[17] Lisovskiy V A and Yegorenkov V D 2004 *Vacuum* **74** 19
[18] Godyak V A and Khanneh A S 1986 *IEEE Trans. Plasma Sci.* **PS-14** 112
[19] Vidaud P, Durrani S M A and Hall D R 1988 *J. Phys. D: Appl. Phys.* **21** 57
[20] Belenguer Ph and Boeuf J P 1990 *Phys. Rev.* A **41** 4447
[21] Boeuf J P and Belenguer Ph 1990 Fundamental properties of RF glow discharges: an approach based on self-consistent numerical models *Nonequilibrium Processes in Partially Ionized Gases* ed M Capitelli and J N Bardsley (New York: Plenum) p 155
[22] Lisovskiy V, Booth J-P, Landry K, Douai D, Cassagne V and Yegorenkov V 2006 *Phys. Plasmas* **13** 103505
[23] Ogle D B and Woolsey G A 1987 *J. Phys. D: Appl. Phys.* **20** 453
[24] Lisovskiy V A and Yegorenkov V D 1998 *J. Phys. D: Appl. Phys.* **31** 3349
[25] Lisovskiy V, Martins S, Landry K, Douai D, Booth J-P and Cassagne V 2005 *J. Phys. D: Appl. Phys.* **38** 872
[26] Lisovskiy V, Martins S, Landry K, Douai D, Booth J-P, Cassagne V and Yegorenkov V 2005 *Phys. Plasmas* **12** 093505
[27] Lisovskiy V, Booth J-P, Martins S, Landry K, Douai D and Cassagne V 2005 *Europhys. Lett.* **71** 407
[28] Nakano N and Makabe T 1995 *J. Phys. D: Appl. Phys.* **28** 31
[29] Shibata M, Nakano N and Makabe T 1995 *J. Appl. Phys.* **77** 6181
[30] Makabe T, Tochikubo F and Nishimura M 1990 *Phys. Rev.* A **42** 3674
[31] Segawa S, Kurihara M, Nakano N and Makabe T 1999 *Japan. J. Appl. Phys.* B **38** 4416
[32] Sommerer T J and Kushner M J 1992 *J. Appl. Phys.* **71** 1654
[33] Lymberopoulos D P and Economou D J 1995 *J. Phys. D: Appl. Phys.* **28** 727
[34] Pitchford L C, Belenguer Ph and Boeuf J P 1993 *Microwave Discharges: Fundamentals and Applications* ed C M Ferreira and M Moisan (New York: Plenum)
[35] Gottscho R A 1987 *Phys. Rev.* A **36** 2233
[36] Lisovskiy V A and Yegorenkov V D 2006 *Vacuum* **80** 458
[37] Iio M, Goto M, Toyoda H and Sugai H 1995 *Contrib. Plasma Phys.* **4–5** 405
[38] Tarnovsky V, Deutsch H, Martus K E and Becker K 1998 *J. Chem. Phys.* **109** 6596
[39] Basner R, Schmidt M, Denisov E, Becker K and Deutsch H 2001 *J. Chem. Phys.* **114** 1170
[40] McDaniel E W 1964 *Collision Phenomena in Ionized Gases* (New York: Wiley)
[41] Lisovskiy V, Landry K, Douai D, Booth J-P, Cassagne V and Yegorenkov V 2007 *J. Phys. D: Appl. Phys.* **40** 6631